Naval Research Laboratory

Washington, DC 20375-5320

NRL/MR/6170--97-8103

Vanadate-sulfate Melt Thermochemistry Relating to Hot Corrosion of Thermal Barrier Coatings

ROBERT L. JONES

Surface Chemistry Branch
Chemistry Division

October 30, 1997

REPORT DOCUMENTATION PAGE

Form Approved
OMB No. 0704-0188

1. AGENCY USE ONLY (*Leave Blank*)	2. REPORT DATE	3. REPORT TYPE AND DATES COVERED
	October 30, 1997	Final Report

4. TITLE AND SUBTITLE

Vandate-sulfate Melt Thermochemistry Relating to Hot Corrosion of Thermal Barrier Coatings

5. FUNDING NUMBERS

PE - 61153N
PE - 62234N

6. AUTHOR(S)

Robert L. Jones

7. PERFORMING ORGANIZATION NAME(S) AND ADDRESS(ES)

Naval Research Laboratory
Washington, DC 20375-5320

8. PERFORMING ORGANIZATION REPORT NUMBER

NRL/MR/6170--97-8103

9. SPONSORING/MONITORING AGENCY NAME(S) AND ADDRESS(ES)

Office of Naval Research
800 North Quincy Street
Arlington, VA 22217-5660

10. SPONSORING/MONITORING AGENCY REPORT NUMBER

11. SUPPLEMENTARY NOTES

12a. DISTRIBUTION/AVAILABILITY STATEMENT

Approved for public release; distribution unlimited.

12b. DISTRIBUTION CODE

13. ABSTRACT (*Maximum 200 words*)

The gas turbine industry is moving strongly toward the use of ZrO_2-based thermal barrier coatings (TBCs) on hot section vanes/blades to increase engine efficiency and durability. In some applications (e.g., ship propulsion or electricity generation), such TBCs may be corroded by molten vanadate-sulfate deposits from fuel impurities. This Report provides a synopsis of vanadate-sulfate thermochemistry relating to TBC hot corrosion, and summarizes research conducted on this topic at the Naval Research Laboratory. The interactions of Na_2O, V_2O_5 and SO_3, the melt components which determine the composition of the vanadate-sulfate deposits, were examined and clarified. Vanadate-sulfate melts were shown to be nonideal rather than ideal—a point of some contention in the past literature—and, for melts of Na/V = 1, to have a V_2O_5 activity coefficient (γ) that ranges from 5×10^{-4} up to essentially 1, depending on the SO_3 overpressure. Different $NaVO_3/Na_2SO_4$ mixtures gave a detectable but small change in $\gamma(V_2O_5)$, suggesting that the Na/V ratio is relatively unimportant, for melts equilibrated with SO_3, in determining $\gamma(V_2O_5)$. The reactions of several candidate ZrO_2 stabilizers (MgO, CeO_2, Sc_2O_3, In_2O_3, SnO_2) with vanadate-sulfate melts are categorized and discussed.

14. SUBJECT TERMS

Hot corrosion; Thermal barrier coatings; Thermochemistry; Vanadate sulfate melts; Gas turbines

15. NUMBER OF PAGES

23

16. PRICE CODE

17. SECURITY CLASSIFICATION OF REPORT	18. SECURITY CLASSIFICATION OF THIS PAGE	19. SECURITY CLASSIFICATION OF ABSTRACT	20. LIMITATION OF ABSTRACT
UNCLASSIFIED	UNCLASSIFIED	UNCLASSIFIED	UL

NSN 7540-01-280-5500

Standard Form 298 (Rev. 2-89)
Prescribed by ANSI Std 239-18
298-102

CONTENTS

VANADATE-SULFATE MELT THERMOCHEMISTRY RELATING TO HOT CORROSION OF THERMAL BARRIER COATINGS

INTRODUCTION

The purpose of this Report is to draw together the knowledge of vanadate-sulfate thermochemistry relating to TBC hot corrosion, including that obtained in work done over several years in Code 6170 of the U.S. Naval Research Laboratory, and to present the total in reviewed form. This is important for several reasons. First, gas turbine technology is now moving toward the wide-spread use of TBCs on the 1st stage turbine vanes/blades (i.e., highly critical components), with many such TBC-fitted engines likely to be used for electricity-generation or other industrial/marine applications where V,S-containing fuels are possible. The hot corrosion of TBCs, and therefore the thermochemistry of vanadate-sulfate melts, may become of concern in these cases. Second, although there have been many thermodynamic studies of metallurgical slags, fused salts, silicate glasses, etc., surprisingly few investigations of vanadate-sulfate melts have been made, despite the long history of vanadate-sulfate hot corrosion (1). And third, among even these few studies, significant differences in findings have been reported. By defining these differences, it may be possible to identify areas in vanadate-sulfate thermochemistry where new research is needed.

Gas Turbine Vane/Blade TBCs

Zirconia is a high temperature thermal insulator, and a ZrO_2 "thermal barrier coating" as thin as 0.010" (0.25 mm) can reduce the temperature between the engine gas and component metal by 100-200°C. Many problems have had to be solved to make TBCs viable (2,3), especially for 1st stage turbine vanes (stationary) and blades (rotating) where large-scale TBC failure could jeopardize engine life. The TBC structure now commonly used for vane/blade applications (Fig. 1) consists of an 0.003-0.005" oxidation-resistant metallic "bond coat" of MCrAlY (where M = Co, Ni, or NiCo) or Pt-aluminide under a ~0.010" layer of Y_2O_3(8-wt%)-ZrO_2 having a columnar, carpet pile-like physical structure. This columnar structure is produced by electron beam-physical vapor deposition (EB-PVD), and is thought to be essential for relieving thermal stress within the TBC, and so yielding long service life.

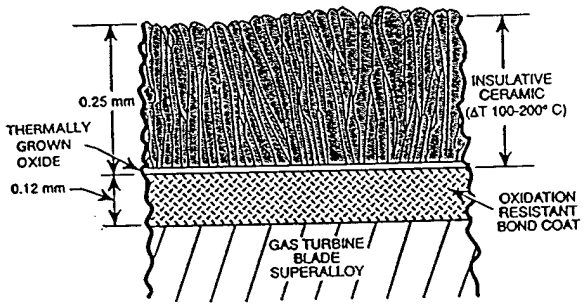

Fig. 1 Schematic drawing of EB-PVD thermal barrier coating.

Significant advantages are claimed for TBCs on vanes/blades, including improved power (up to 20%), fuel economy (several percent), and/or component life (up to 3X improvement). For example, in land-based gas turbines, an increase of 55°C in turbine gas temperature is expected to provide an 8 to 13 percent gain in power, and a 1 to 4 percent increase in simple cycle efficiency (4). The faith of the gas turbine industry in TBC technology is shown by the fact that many $10s of millions of dollars have been spent by such companies as United Technologies (Pratt & Whitney Aircraft Engines), General Electric Aircraft Engine Company, Chromalloy Corp., and Praxair Surface Technologies to purchase production-scale, EB-PVD coaters for application of TBCs to aviation and industrial gas turbine vanes/blades.

Manuscript approved September 19, 1997.

Combined Cycle Gas Turbines for Electricity Generation

A world-wide movement is underway, as exemplified in the U.S. Dept. of Energy 8-year, $700M Advanced Turbine Systems (ATS) Program (5), to use high efficiency gas turbines in combined cycle with bottoming steam turbines to produce electricity with up to 60% thermal efficiency. Such plants would require approximately 50% less fuel than present-day fired boiler plants which have 35-42% thermal efficiency. Moreover, since these plants are intended mostly to burn natural gas, which normally consists of 90% or more of methane (CH_4), there would be proportionately less CO_2 released to the environment than with fuels of higher C/H ratio.

To achieve high fuel efficiency, the massive electricity-generating gas turbines (with power in ranges of up to 250-300 MW) will employ the latest gas turbine technology, with many using single crystal blades (despite their large size) and TBC coated vanes/blades. Because of the possibility of future high prices, or shortages, in natural gas, these engines must have the back-up capability for firing with industrial-grade petroleum fuel. The vane/blade TBCs must therefore have the ability to withstand at least certain levels of vanadium and sulfur fuel impurities, even though the high surface temperatures for TBCs may tend to reduce deposit accumulation. Also, it is common in less developed countries to burn locally-produced industrial or crude oils that may contain significant vanadium or sulfur, and engine manufacturers are seeking vane/blade TBCs that can be used, with economic advantage, even in these circumstances.

Vanadium in Petroleum

Vanadium occurs in most crude oils, and in some cases, at levels up to 500 ppm (6). The vanadium is mostly complexed as heavy metalloporphyrin molecules, and tends to remain in the residual during refining; however, since metalloporphyrins are slightly volatile at higher temperatures, some vanadium may also be found in the higher-boiling distillate fuels.

Vanadium (as V_2O_5) accumulates on, and deactivates, the catalysts used in the fluid catalyst cracking of petroleum. Much effort has been spent to alleviate this problem, which is now mostly approached by catalyst modification, or metals passivation where certain metals such as Sb or Sn are added to the feedstock to "passivate" the catalyst against V_2O_5 attack (6,7). Vanadium also interferes with the hydrogen-desulfurization (HDS) of high-sulfur crudes by depositing on the catalyst. To remove vanadium itself, refiners can use an aggressive hydrogen treatment over catalysts (hydrodemetallization or HDM), as well as coking or other means (6). Approximately 2,650 metric tons of vanadium were recovered and marketed in the US from petroleum residues in 1996 (8). The treatments for removing vanadium are sophisticated and expensive, however, and may not be routinely performed in refining, especially in less developed countries.

Previous Studies of Vanadate Hot Corrosion of TBCs

During the fuel crises of the 1970s, the U.S. Dept. of Energy investigated alternative sources of liquid fossil fuel (coal liquefaction, etc.), as well as means for improving engine fuel economy (e.g., thermal barrier coatings). The possible corrosive attack of TBCs by low-quality alternate fuel containing vanadium, phosphorus, sulfur, etc. was investigated under DOE contract by several engine companies including Westinghouse, General Electric, Solar Turbines and others. The results from these studies were primarily published in two Conference Proceedings (9,10) jointly sponsored by DOE and EPRI (Electric Power Research Institute).

The DOE-sponsored studies focused essentially on MgO(20-25wt%)-ZrO_2 (MSZ) and Y_2O_3(8-20wt%)-ZrO_2 (YSZ) thermal barrier coatings. MSZ was found to lack high temperature phase stability, and to be destabilized simply by thermal cycling to 1000°C. The MgO stabilizer, although somewhat

more resistant to reaction with V_2O_6 than Y_2O_3, reacted readily with SO_3 to form $MgSO_4$, and was strongly leached from MSZ by the SO_3 in burner rigs burning 1wt%-S fuel. YSZ was clearly superior, and exhibited good 1000°C phase stability, as well as resistance to reaction with Na_2SO_4-SO_3 at the SO_3 partial pressures found in engines burning fuel of 1-2% S levels. However, Y_2O_3 was confirmed by many as being highly reactive with V_2O_6, even when the Y_2O_3 was at reduced activity as 8-wt% (4.5 mol%) Y_2O_3 in solid solution in ZrO_2.

Building upon the original DOE-funded work, the U.S. Naval Sea Systems Command sponsored research to explore the potential of TBCs for vane/blade use in the General Electric LM2500 gas turbine which powers several important classes of Navy ships. Burner rig tests, along with one limited engine test, indicated that coatings of Y_2O_3(8-wt%)-ZrO_2 in fact resisted $NaSO_4$-SO_3 hot corrosion better than the metallic MCrAlY or Pt-aluminide coatings normally used for corrosion protection (11). There was also no evidence of molten salt penetration into the intergranular spacings of the EB-PVD prepared thermal barrier coatings. The relative performance of MgO-, CeO_2-, and Y_2O_3-stabilized ZrO_2 TBCs was evaluated in another burner rig test series, which used fuel contaminated with vanadium (up to ~90 ppm), sea salt, and sulfur (12). MgO-ZrO_2 was judged to be by far the most reactive, whereas CeO_2-ZrO_2 and Y_2O_3-ZrO_2 were judged to perform moderately well (in terms of the TBC not spalling). All showed chemical reactivity, however, with MgO forming large amounts of $MgSO_4$, and CeO_2 and Y_2O_3 each forming vanadates, although with some sulfate. The formation of cerium vanadate ($CeVO_4$) was somewhat unexpected, since CeO_2 shows some resistance to V_2O_6 reaction (see below), but this may have resulted because of the relatively high concentrations of vanadium and sulfur used.

THERMOCHEMISTRY OF VANADATE-SULFATE MELTS: REVIEW AND DISCUSSION

The principal driving force for the degradation of TBCs by hot corrosion is chemical reaction between the stabilizing oxides (e.g., Y_2O_3, CeO_2, etc.) and the molten vanadate-sulfate engine deposits, or essentially vanadate-sulfate melts. Vanadium-containing melts of relatively low V_2O_6 activity (e.g., $NaVO_3$) can cause phase reversion in CeO_2-ZrO_2 TBCs (and possibly In_2O_3-ZrO_2 TBCs) by a "mineralization" effect where no chemical reaction of the CeO_2 can be detected (13). However, this is of second magnitude compared to hot corrosion chemical reaction. The thermochemistry of the vanadate-sulfate melt determines whether chemical reaction, or corrosion, of the TBC components will occur, and it is thus the ultimate factor in deciding TBC life in corrosive environments.

Mechanism of Vanadate Hot Corrosion of Y_2O_3-ZrO_2 TBCs

As established in DOE-sponsored research (9), and since verified by others, the attack of vanadium on yttria-stabilized zirconia (YSZ) thermal barrier coatings occurs by:

$$Y_2O_3 \text{ (in solid soln in } ZrO_2) + V_2O_6 \text{ (l)} = 2\ YVO_4 \text{ (s)} + ZrO_2 \text{ (s, monoclinic)} \quad [1]$$

where Y_2O_3 in solid solution in the ZrO_2 matrix reacts with the V_2O_6 (l) component of the vanadate-sulfate engine deposit to produce highly stable, solid YVO_4 (mp 1810°C) and solid ZrO_2, but with the ZrO_2 being destabilized and in the monoclinic phase structure. No chemical reaction of V_2O_6 with ZrO_2 is normally detected. Reaction [1] can be confirmed by heating thin deposits of $NaVO_3$ on sintered YSZ pellets, where one then sees masses of acicular YVO_4 crystals formed on the YSZ surface by outward diffusion of Y_2O_3, while destabilized monoclinic ZrO_2 is left below (14). Specific details of the crystallographic orientation of YVO_4 growing on YSZ have been revealed by thin film TEM (15), while the diffusion of V_2O_6 and Y_2O_3 within YSZ has been studied by Rutherford back-scattering (16).

The activity of V_2O_6 (l) determines whether reaction [1] will occur, since YVO_4 and ZrO_2 are pure solids (activity = 1), and although Y_2O_3 is in solid solution in ZrO_2 (act. < 1), its activity is fixed until reaction [1] actually commences. It is important therefore to know the V_2O_6 activity in vanadate-

sulfate engine deposits to predict when reaction [1] is possible, and to evaluate alternative stabilizers for improving the hot corrosion resistance of TBCs. As an example, the activity coefficient (γ) for 0.045 mol-fraction (8-wt%) of Y_2O_3 in ZrO_2 at 2500°C has been measured as ~0.1 (17), and is probably lower at 800-900°C (assume 0.01), since negative deviation from ideal solution behavior normally increases with decreasing temperature. Using the assumed $\gamma(V_2O_5)$ of 0.01, one can obtain an approximation of the act.(V_2O_5) at which reaction [1] should commence by thermodynamic calculation using Gibbs energy data provided by Yokokawa et al (18), viz.,

$$\Delta G^\circ_{800C} = \sum \Delta_f G^\circ_{pdts} - \sum \Delta_f G^\circ_{reagents} = -RT \ln K \qquad [2]$$

$$K = \frac{(act.YVO_4)^2 \times (act.\ ZrO_2)}{(act.V_2O_5) \times (act.Y_2O_3)} = 1.803 \times 10^{11} = \frac{1}{(4.5 \times 10^{-4}) \times (act.V_2O_5)}$$

or, therefore act.(V_2O_5) $\geq$ 1.2×10^{-6} for reaction [1] to occur

This value of act.(V_2O_5) is exceeded by the act.(V_2O_5) of ~10^{-4} found for $NaVO_3$ at 850°C (see below), and therefore it is consistent that YSZ reacts readily with molten $NaVO_3$ ($Na_2O.V_2O_5$), but not with the more basic Na_3VO_4 ($3Na_2O.V_2O_5$), as found in the next section.

Lewis Acid/Base Reaction of Ceramic Oxides with Sodium Vanadates

Fig. 2 shows the reaction behavior of a number of oxides of increasing acidity as these are heated at 700-900°C with vanadium compounds of increasing acidity; i.e., Na_3VO_4 ($3Na_2O.V_2O_5$), $NaVO_3$ ($Na_2O.V_2O_5$), and pure V_2O_5 (19). Two important aspects of Fig. 2 should be noted. First, the reactions are primarily controlled by the Lewis acid/base nature of the oxide, with no reaction occurring when the Lewis basicities are approximately equal. A compound such as $NaVO_3$ can react as an acid, providing V_2O_5, with an oxide of the basicity of Y_2O_3, but as a base, providing Na_2O, with oxides of the acidity of GeO_2 or Ta_2O_5.

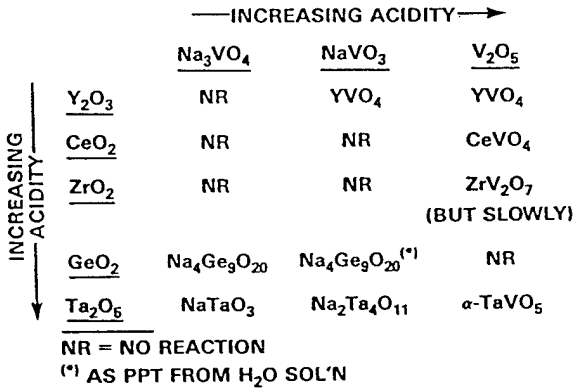

Fig. 2 Lewis acid/base reaction of selected oxides with sodium vanadates and V_2O_5.

Second, the ceramic oxides react with either the Na_2O or V_2O_5 component of the sodium vanadate compounds, and not with the compounds themselves. The role of the sodium vanadate compound is only to make Na_2O or V_2O_5 available at some certain level of activity. The reaction products consist of multiples of Na_2O or V_2O_5 with the various oxides, as for example, $2Na_2O.9GeO_2$, $Na_2O.2Ta_2O_5$, $Y_2O_3.V_2O_5$ (i.e., 2 YVO_4), etc. An exception to this rule was found in later experiments with Sc_2O_3, which reacts with $NaVO_3$ to form $3NaVO_3.Sc_2O_3$ at temperatures below 880°C (20). The oxidation state of the different cations does not change, except for the case of CeO_2 where Ce^{4+} goes to Ce^{3+} during the formation of $CeVO_4$ (see below).

Previous Studies of Vanadate-Sulfate Thermochemistry

Although numerous publications on vanadate-sulfate hot corrosion can be found in the literature, only four pertain to the actual thermochemistry of vanadate-sulfate deposits. These are listed in Table 1.

TABLE 1

Past Studies of the Thermochemistry of Vanadate-Sulfate Melts

Year	Authors/Reference	Topic/Conclusions
1982	Luthra & Spacil, Ref. 21	Thermodynamic calculation of Na,V,S deposition in gas turbines; found $\gamma(V_2O_6)$ of 0.18 and 0.08 at 750° and 900°C for Na/V = 2 and 8.7×10^{-4} and 3.6×10^{-4} $p(SO_3)$, resp.
1984	Mittal & Elliott, Ref. 22	Electrochemical study of Na_2O-V_2O_6 melts, with Na_2O activity by electrode EMF, V_2O_6 activity by Gibbs-Duhem integration; melts found to be highly nonideal
1989	Hwang & Rapp, Ref. 23	Calculation of Na_3VO_4, $NaVO_3$ and V_2O_6 concentrations in melts; vanadate-sulfate melts assumed to be ideal; predicted ~20% V^{4+} in Na-V melts at 900°C and -log Na_2O of 15.3~18.7
1995	Reidy & Jones, Ref. 24	TGA study of SO_3 equilibrium with $NaVO_3$ at 800°C, and reaction of melt with CeO_2; for lowest V_2O_6 levels, found $\gamma(V_2O_6) \approx 0.01$

Question of V^{4+}/V^{5+} in Vanadate-Sulfate Melts

In the older boiler corrosion research (1), it was postulated by many that vanadium-rich deposits contained V^{4+}/V^{5+} couples which transported oxygen by reactions of the type:

$$Na_2O.V_2O_4.5V_2O_6 + 1/2\ O_2 \rightleftarrows Na_2O.6V_2O_6 \qquad (3)$$

where one could have

$$Na_2O.V_2O_4.5V_2O_6 + SO_3 \rightarrow Na_2O.6V_2O_6 + SO_2 \qquad (4)$$

which might then be followed by

$$Na_2O.6V_2O_6 + Fe \rightarrow Na_2O.V_2O_4.5V_2O_6 + FeO \qquad (5)$$

One solution proposed for vanadate-induced corrosion by heavy oils in boilers was the use of "low excess air", or LEA. In pilot boiler tests (25) using low-quality oil containing 2.57 wt% S, 53 ppm Na, and 350 ppm V, the vanadium in boiler-tube deposits forming at 1300°F (704°C) was 91% V_2O_6, 9% V_2O_3 and/or V_2O_4 with 15% excess air, but only 24% V_2O_6 with 76% V_2O_3 and/or V_2O_4 at 1% excess air. In the latter instance, there was significantly lower deposit formation and boiler-tube corrosion, presumably because of the higher melting points and physical nature of V_2O_3 and V_2O_4. These data therefore indicate that V_2O_3 or V_2O_4 can be found in boiler deposits. However, this occurs under nearly reducing combustion conditions, and also where there is the possibility of V_2O_6 reduction by tube metal oxidation (the 1300°F tube deposits in fact consisted of about 75% corrosion product).

Whether V^{4+} would occur in significant amounts in vanadate-sulfate melts on TBCs in gas turbines operating at high air/fuel ratios, or in laboratory studies of vanadate-sulfate melts under ambient O_2 partial pressures, is another question. In these cases, the conditions are oxidizing, and the ceramic oxides involved (ZrO_2, Y_2O_3, etc.) are stable to very low $p(O_2)$, except for CeO_2 which, as the pure oxide at 1000°C, begins to be reduced to $CeO_{1.83}$ at $\sim 10^{-12}$ atm of O_2. Calculations by Hwang and Rapp (23) indicate that Na_2SO_4-30 mol% $NaVO_3$ melts at 900°C and ambient $p(O_2)$ should contain ~20% V^{4+} over the log act.(Na_2O) range of -15.3 to -18.7. However, this contradicts the findings of Mittal and Elliott (22) who conclude that vanadium in liquid Na_2O-V_2O_5 exists only as V^{5+} over the measured log act.(Na_2O) range of -13 to -20 at 852°C (see below). They support their conclusion by citing Block-Bolton and Sadoway (26) who found no V^{4+} in liquid V_2O_5 at 1200K (927°C) for $p(O_2) >$ 0.06 atm. Also, it appears that Na_2O stabilizes V^{5+} in V_2O_5, as proposed by Mittelstadt and Schwerdtfeger (27) who observed that whereas $Na_2O.5V_2O_5$ begins to reduce to V^{4+} at 10^{-2} atm $p(O_2)$ at 1000°C, $Na_2O.V_2O_5$ is stable down to 10^{-5} atm $p(O_2)$.

As another consideration, when CeO_2 reacts with the V_2O_5 component of vanadate-sulfate melts (see below), the reaction goes as,

$$2\ CeO_2\ (s) + V_2O_5\ (l) \rightarrow 2\ CeVO_4\ (s) + 1/2\ O_2\ (g) \qquad [6]$$

A reduction occurs in reaction [6], but one can not be certain, a priori, whether it is the cerium cation (4^+ to 3^+) or the vanadium cation (5^+ to 4^+) that is reduced. To answer this question, Reidy and Swider (28) examined $CeVO_4$ by X-ray absorption spectroscopy (XAS) and showed that cerium is in the Ce^{3+} state in $CeVO_4$, and vanadium thus in the V^{5+} state. Taken overall, the literature data indicate that, for the oxidizing conditions postulated, V^{4+} is unlikely to be significant in the thermochemistry of vanadate-sulfate melts relating to TBC ceramic hot corrosion.

Thermodynamic Modeling of Acid-Base Melts

The activity of a component of a solution or melt is defined according to

$$\text{act.} = \gamma \times X \qquad [7]$$

where act. is the component activity, γ is the activity coefficient, and X is the mol-fraction of the component. For ideal solutions, the activity coefficient is unity, and the activity of a component is simply equal to its mol-fraction. Almost all melt solutions are nonideal, however, and in that case, γ changes with the overall composition of the solution. To describe how γ varies with melt composition, solution scientists often adopt "solution models" which, following theoretical or empirical reasoning, are intended to predict the dependence of γ on melt composition.

Many solution models have been developed since, in different types of melts, the melt components interact in different ways, which must be taken into account. For oxide systems which involve strong acid-base chemical interactions (such as at present), the best model appears to be the Ideal Mixing of Complex Components (IMCC) model developed by Bonnell and Hastie (29). This model is capable of describing the very large changes in the ratio of formal concentration to thermodynamic activity (10^{10} or more) that can occur in strong acid-base reactions, as demonstrated by Bonnell and Hastie for complex slags containing such components as Na_2O, SiO_2, K_2O, and Al_2O_3.

The IMCC model uses Gibbs-energy-minimization by computer to determine the "free" mol-fraction, as opposed to the nominal mol-fraction, of a component such as K_2O, when that component exists in the melt in competing equilibria with other components by reactions such as,

$$K_2O + SiO_2 \rightleftarrows K_2SiO_3 \qquad [8]$$

$$K_2SiO_3 + SiO_2 \rightleftarrows K_2Si_2O_5 \quad [9]$$

$$K_2Si_2O_5 + 2\ SiO_2 \rightleftarrows K_2Si_4O_9 \quad [10]$$

It is thus akin to the NASA-developed computer calculation of the equilibria of molecular species in high temperature gases, and also to the calculations made for the Na_2O-V_2O_5-SO_3 system by Luthra and Spacil (21). The IMCC model assumes ideal mixing of the various "product molecules" once they have been formed by the chemical reactions indicated; that is, there is assumed to be no other type of interaction between the product molecules, after they are formed, that would yield significant additional Gibbs energy of solution for the melt.

This raises the question of whether such "product molecules" actually exist in melts. For gases, techniques such as high temperature mass spectrometry, infrared spectroscopy or gas chromatography can be used to identify gas phase molecules, and, if conditions are such that kinetics do not interfere, the thermodynamically-predicted gaseous species generally are found, and in the approximate quantities calculated. With melts, however, it is not possible to make an equivalent molecular identification of melt species. About the best information available is obtained with binary metal melts such as Sb-Mg, where plotting the excess solution stability (d^2G^E/dx_1^2, where G^E is the excess integral molar free energy of a solution) against melt composition may reveal peaks at certain stoichiometries which indicate the formation of melt complexes such as Mg_3Sb_2 (30). Bonnell and Hastie (29) approach this problem by considering that "-- the liquid components are not necessarily independent molecular or ionic species, but serve to represent the local associative order." The goodness of fit between solution model prediction and experimental results obtained by Bonnell and Hastie appears to justify their hypothesis, although it remains difficult to envision the arrangement of atoms in the melt that this would imply.

For the purposes of the present Report, the discussion in this section has mostly only philosophical implications, since no solution model for the Na_2O-V_2O_5-SO_3 system is proposed from our NRL research. The NRL results do contain, however, substantial experimental data (see below) that could be used in the development of such a solution model.

Study of Na_2O-V_2O_5 Melts by Mittal and Elliott

Mittal and Elliott (22) consider sodium vanadate deposits to be mixtures of vanadium oxide (V_2O_5) and sodium oxide (Na_2O) produced by oxidation of Na,V-impurities in fuel during combustion. Our NRL research has taken the same approach, but with the effect of engine gas SO_3 added in. Since the Mittal and Elliott paper in some ways represents the "starting point" for our NRL work, their paper will be discussed in detail here.

Mittal and Elliott made electrochemical measurements at 757-937°C of the activity of Na_2O in melts having a V_2O_5 mol-fraction range of 0.5 to 0.9; that is, totally molten mixes from $Na_2O.V_2O_5$ (i.e., $NaVO_3$) up to $Na_2O.9V_2O_5$ in the V_2O_5-rich half of the Na_2O-V_2O_5 phase diagram (Fig. 3). These composition and temperature

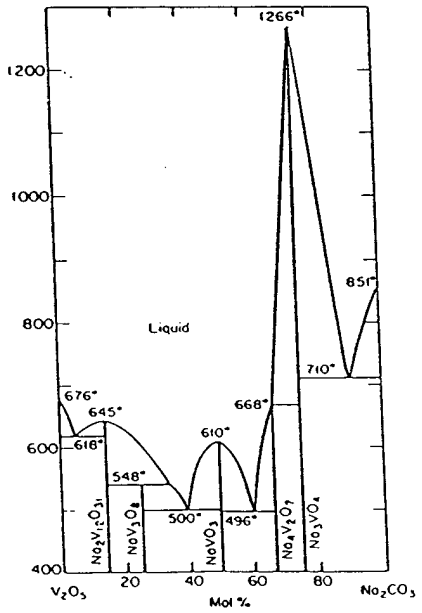

Fig. 3 Phase diagram for V_2O_5-Na_2CO_3 (Na_2O). Ref. 31.

ranges are generally thought to be among the most corrosive in terms of vanadate hot corrosion. The corresponding activities for V_2O_6 were calculated by integration of the Gibbs-Duhem equation.

The activities of Na_2O and V_2O_6 found by Mittal and Elliott for molten Na_2O-V_2O_6 mixes at 852°C (1125K) are plotted in Fig. 4. At 0.5 mol-fraction of V_2O_6 (that is, for $Na_2O.V_2O_6$ or $NaVO_3$), the log of Na_2O activity is -13.13, and that of V_2O_6 is -3.62, giving a log activity product of -16.75. This value can be compared with thermodynamic calculation for the reaction,

$$2\ NaVO_3\ (l) \rightleftarrows Na_2O\ (l) + V_2O_6\ (l) \qquad [11]$$

where the log activity product of Na_2O and V_2O_6 is found to be -16.93, using thermodynamic data by Yokokawa et al (18) and Barin (32). This is good agreement which supports the Mittal and Elliott results as being correct.

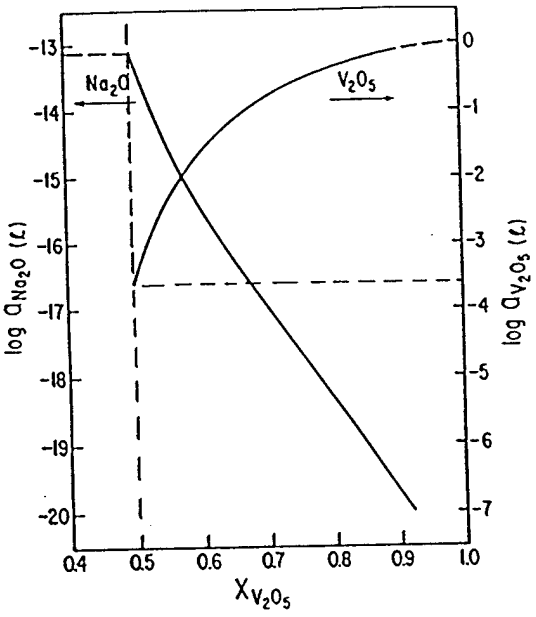

Fig. 4 Log act.(Na_2O) and log act.(V_2O_6) in the Na_2O-V_2O_6 binary system at 1125 K (852°C). From Ref. 22.

The data of Mittal and Elliott are plotted in Fig. 5 with Na_2O and V_2O_6 as the melt components. This plotting shows V_2O_6 to have a strong negative deviation from ideal solution behavior. The V_2O_6 activity coefficient for $X(V_2O_6) = 0.5$ (i.e., in molten $NaVO_3$) is $\sim 4.8 \times 10^{-4}$, as obtained by dividing the V_2O_6 activity, log -3.62, by the V_2O_6 mol-fraction concentration, 0.5. The Mittal and Elliott data can also be recalculated and plotted to reflect $NaVO_3$ and V_2O_6 as being the melt components. This yields Fig. 6, where V_2O_6 continues to exhibit a negative deviation from ideal solution behavior. Fig. 6 indicates therefore that $NaVO_3$ and V_2O_6 do not mix in a totally ideal fashion, as assumed in the calculations by Hwang and Rapp (23). As a final

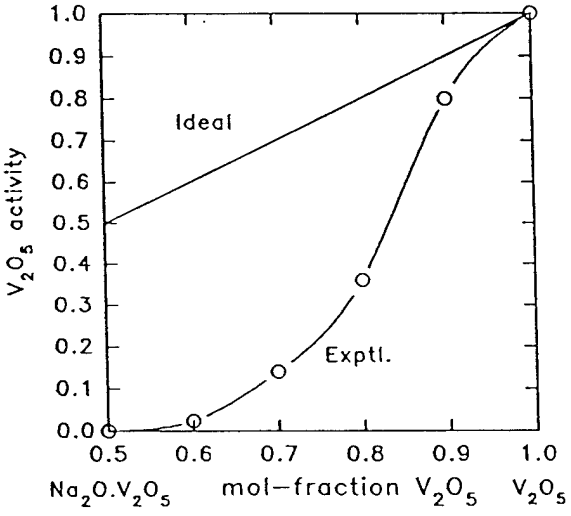

Fig. 5 Solution behavior of Na_2O-V_2O_6 at 852°C, taking Na_2O and V_2O_6 as the melt components.

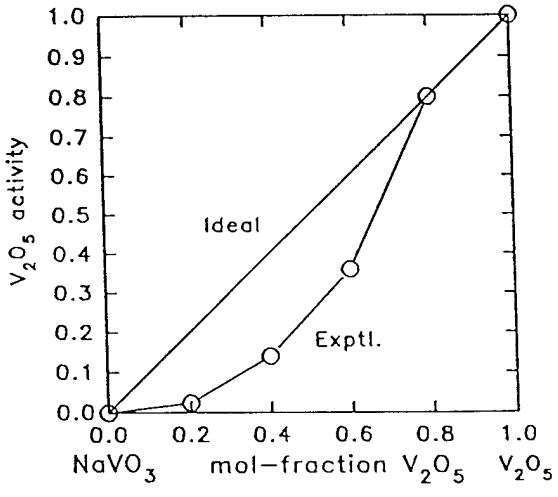

Fig. 6 Solution behavior of Na_2O-V_2O_6 at 852°C, with $NaVO_3$ and V_2O_6 as the melt components.

side point, notice that there are no obvious inflections in the experimental log act.(Na_2O) curve of Mittal and Elliott (Fig. 4) such as might reflect any influence in the melt behavior resulting from the compounds, $Na_2O.3V_2O_5$ (NaV_3O_8) and $Na_2O.6V_2O_5$ ($Na_2V_{12}O_{31}$), which occur within the Na_2O-V_2O_5 composition range studied (Fig. 3).

Thermogravimetric Equilibrium of SO_3 with $NaVO_3$ Melts

The mutual interaction between Na_2O, V_2O_5 and SO_3, as occurs in engine vanadate-sulfate deposits, was investigated by a thermogravimetric technique in which SO_3 at increasing partial pressures was equilibrated with molten $NaVO_3$ at 800°C. The reaction is described by,

$$2\ NaVO_3\ (l) + SO_3\ (g) \rightleftarrows V_2O_5\ (l) + Na_2SO_4\ (l) \qquad [12]$$

Reaction [12] was identified by Luthra and Spacil (21) as being the major reaction in determining the composition of vanadate-sulfate engine deposits under marine gas turbine conditions. Also, we have shown earlier that whereas CeO_2 does not react chemically with pure molten $NaVO_3$, an overpressure of SO_3 yields V_2O_5 by reaction [12], with $CeVO_4$ then forming by reaction between CeO_2 and V_2O_5 (19). Note that one starts with pure $NaVO_3$ in reaction [12] and then essentially adds, by using initially very low partial pressures of SO_3, small increments of V_2O_5 and Na_2SO_4 to the original $NaVO_3$. The thermochemical behavior of the resultant melts would therefore be expected to show a smooth transition from the thermochemical properties found by Mittal and Luthra for 0.5 mol-fraction Na_2O-V_2O_5 ($NaVO_3$), at least for the initial low V_2O_5- and Na_2SO_4-content mixes.

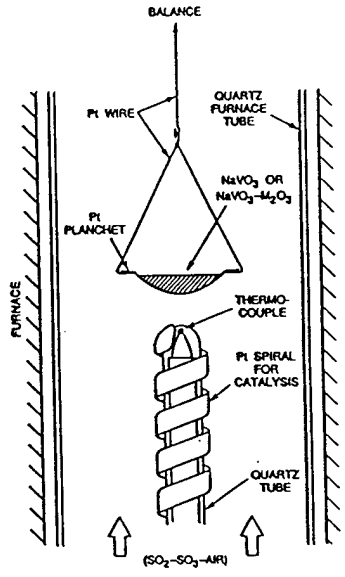

Fig. 7 Arrangement of specimen melt planchet (Pt) within furnace.

Our thermogravimetric analysis (TGA) furnace system used a two-stage gas dilution arrangement which employed electronic mass flow gas controllers to give SO_2 partial pressures of down to 10^{-8} bar in the furnace input air (33). The SO_2/air input mixture was equilibrated over Pt at temperature in the furnace (Fig. 7), with the SO_3-SO_2-air mixture then passing over the $NaVO_3$ melt (50 mg) which was contained in a shallow, balance-suspended Pt planchet. After an initial weight loss of ~2% (the $NaVO_3$ contained about 2% water), the system showed negligible weight change (< 0.2 mg) for periods in excess of 50 hrs under slowly flowing (50 ml/min) air dried over Drierite™.

Attainment of SO_3 equilibrium. As the $p(SO_3)$ was lowered, the time required to reach equilibrium became progressively longer, so that for $p(SO_3) \leq 10^{-6}$, 100 hrs or more would be needed for equilibrium by simple exposure to the test $p(SO_3)$. Our procedure therefore was to bring the $NaVO_3$ to both above and below equilibrium weight (in separate measurements) at a higher $p(SO_3)$, and then return the system to the test $p(SO_3)$ and monitor the wgt gain vs. time slopes (positive or negative), which were back-extrapolated to identify the true equilibrium weight (33). The time for equilibrium also was found to be proportional to the weight of $NaVO_3$, taking approximately twice as long for 100 mg as 50 mg $NaVO_3$. This experience raises the question, at least in the author's mind, of how massive amounts of melt (up to 25 gms) in a narrow electrochemical cell could become equilibrated with low $p(SO_3)$'s ($\leq 10^{-4}$ atm) in a reasonable time. Two possible answers come to mind: first, many

of the electrochemical experiments were at 900°C rather than 800°C as here, and the 100°C higher temperature may significantly speed up SO_3 diffusion; second, our melt is, at least initially, pure $NaVO_3$, whereas most electrochemical experiments involving SO_3 equilibrium use melts consisting mostly of sulfates, and it may be that SO_3, perhaps as $S_2O_7^-$, diffuses more rapidly through sulfate-based melts than vanadate-based melts.

Thermodynamic Analysis of SO_3-$NaVO_3$ Equilibrium Data

The equilibrium weight gain data for 50 mg (0.41 mmols) of dried $NaVO_3$ under different $p(SO_3)$ at 800°C are presented in Fig. 8. The weight gain behavior was reversible and reproducible (to within ±0.2 mg), which confirms that SO_3 is absorbed, or given off, without any permanent change in the $NaVO_3$ melt. Conversion of the $NaVO_3$ completely to Na_2SO_4 and V_2O_5 by reaction [12] would yield an equilibrium weight gain of 16.4 mg.

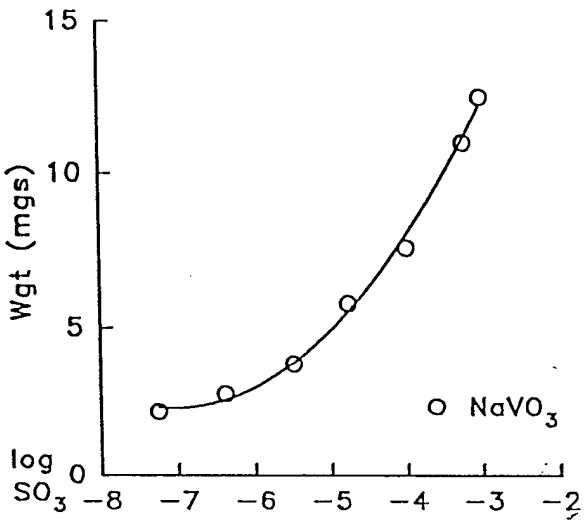

Fig. 8 Weight gain behavior of $NaVO_3$ equilibrated at 800°C with the indicated SO_3 partial pressures.

From the weight gain and stoichiometry of reaction [12], one can calculate the mol-fraction of V_2O_5 experimentally formed at each $p(SO_3)$, as listed in Table 2. And, since the activity coefficient equals unity for ideal solutions and therefore act. = X, the "ideal" mol-fraction can be calculated from thermodynamic data following the procedure outlined in reaction [2]. Using the thermodynamic data provided by Luthra and Spacil (21) for the reagents and products in reaction [12], one obtains,

$$K = 91.61166 = \frac{act.(V_2O_5) \times act.(Na_2SO_4)}{act.(NaVO_3)^2 \times p(SO_3)} \qquad [13]$$

which, by transposing $p(SO_3)$ and setting act. = X, reduces to a quadratic equation in the unknown, x, that can be solved by numerical approximation on the computer for each $p(SO_3)$,

$$91.61166 \times p(SO_3) = \frac{x^2}{(1-2x)^2} \qquad [14]$$

The "ideal" mol-fractions (or "ideal" activities) for V_2O_5 so obtained are listed in Table 2. Division of the ideal V_2O_5 mol-fraction by the experimental V_2O_5 mol-fraction then yields an approximate $\gamma(V_2O_5)$, listed in Table 2 as "$\gamma(V_2O_5)$-Approx. 1" for each $p(SO_3)$, or alternatively, for each melt composition.

However, approximation 1 for $\gamma(V_2O_5)$ is not correct since the actual value for act.(V_2O_5) has not been determined. Approximation 1 treats $NaVO_3$, Na_2SO_4 and V_2O_5 as all behaving ideally, which is almost certainly not true. Luthra and Spacil (21), for example, considered $NaVO_3$ and Na_2SO_4 to be ideal, but V_2O_5 to be nonideal because of its stronger interactions with the melt. If V_2O_5 is assumed nonideal, while $NaVO_3$ and Na_2SO_4 are ideal, then equation [14] can be modified to give, using the experimentally-determined mol-fractions, a second approximation for $\gamma(V_2O_5)$ according to,

$$\gamma(V_2O_6)\text{-Approx. 2} = \frac{91.61166 \times p(SO_3) \times X(NaVO_3)^2}{X(Na_2SO_4) \times X(V_2O_6)} \quad [15]$$

The values for $\gamma(V_2O_6)$-Approx. 2 are listed in Table 2, with both approximations being plotted in Fig. 9. Inspection of Fig. 9 suggests that $\gamma(V_2O_6)$-1 is probably closer to correct at the higher $p(SO_3)$, while $\gamma(V_2O_6)$-2 is more nearly correct at the lower $p(SO_3)$ values. This may be partially explained along the following lines. Note in equation [13] that at the lowest $p(SO_3)$, $NaVO_3$ is almost pure, and its activity thus essentially 1. Under these circumstances, K x $p(SO_3)$, a known value, becomes equal to the activity product, i.e., act.(V_2O_6) x act.(Na_2SO_4). Determining act.(V_2O_6) is then a matter of correctly apportioning the activity product. In Approx. 1, all species are treated as ideal, and act.(V_2O_6) = act.(Na_2SO_4), with act.(V_2O_6) being therefore simply 1/2 of the activity product. In Approx. 2, where Na_2SO_4 (l) but not V_2O_5 (l) is assumed ideal, act.(Na_2SO_4) = X(Na_2SO_4), and division of the activity product by X(Na_2SO_4) from Table 2 yields a lower activity for the "nonideal" V_2O_5 Species. In actuality, Na_2SO_4 (l) is probably not totally ideal, and act.(V_2O_6) should fall somewhere between the Approx. 1 and Approx. 2 values. One might expect also that, as their mol-fraction concentration increases at high $p(SO_3)$, V_2O_5 and Na_2SO_4 would exhibit activity coefficients closer to unity (cf. Fig. 5), making Approx. 1 more nearly correct. Therefore, for purposes of a later comparison (see below), an averaged $\gamma(V_2O_6)$ was calculated, which is shown as $\gamma(V_2O_6)$-Avg in Fig. 9. The calculated average is weighed toward $\gamma(V_2O_6)$-2 at the lower $p(SO_3)$, and $\gamma(V_2O_6)$-1 at the higher $p(SO_3)$.

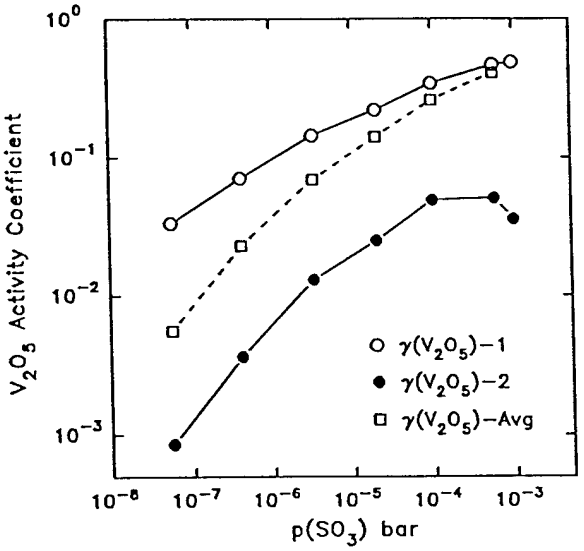

Fig. 9 Values for $\gamma(V_2O_6)$, Approxs. 1 and 2, and $\gamma(V_2O_6)$-Avg. plotted against $p(SO_3)$.

TABLE 2

Experimental Results and Calculated Approximations for $\gamma(V_2O_6)$ in $NaVO_3$ Equilibrated with SO_3 at 800°C

$p(SO_3)$ in bar	Wgt. gain in mg	Exptl. X(V_2O_6)	"Ideal" X(V_2O_6)	$\gamma(V_2O_6)$-Approx. 1	$\gamma(V_2O_6)$-Approx. 2	$\gamma(V_2O_6)$-Avg.
5.6×10^{-8}	2.2	0.0670	0.00225	0.0336	8.6×10^{-4}	0.0055
4.1×10^{-7}	2.8	0.0853	0.00603	0.0707	3.6×10^{-3}	0.023
3.3×10^{-6}	3.8	0.116	0.0167	0.144	1.3×10^{-2}	0.069
2.0×10^{-5}	5.8	0.177	0.0392	0.221	2.5×10^{-2}	0.14
1.0×10^{-4}	7.6	0.232	0.0799	0.344	4.9×10^{-2}	0.26
5.8×10^{-4}	11.0	0.335	0.157	0.469	5.1×10^{-2}	0.41
9.9×10^{-4}	12.5	0.381	0.186	0.488	3.6×10^{-2}	0.49

Note that the $\gamma(V_2O_6)$ values in Table 2 depend, of course, upon the thermochemical data selected. If data incorporating values provided more recently by Yokokawa et al (18) are used, the value of K is raised from 91.61166 to 168.8 which, for example at $p(SO_3) = 5.6 \times 10^{-8}$ bar, changes $\gamma(V_2O_6)$-Approx. 2 for from 8.6×10^{-4} to 1.6×10^{-3}.

Reaction of Candidate Stabilizing Oxides with SO_3-$NaVO_3$

The equilibrated SO_3-$NaVO_3$ TGA technique was used to investigate the reaction of MgO, Y_2O_3, Sc_2O_3 and In_2O_3 (33), Cr_2O_3 and SnO_2 (34), and CeO_2 (24) with the Na_2O-V_2O_6-SO_3 melt system, with the mix ratio of 0.41 mmols $NaVO_3$ and 0.1 mmols of oxide normally being employed. As summarized in Fig. 10a-10g, the results serve to rank the potential vanadate-sulfate hot corrosion resistance of candidate stabilizing oxides for ZrO_2. They also provide information about the nature of the different reactions that the various oxides undergo with vanadate-sulfate melts. These can be broken down into categories as described below:

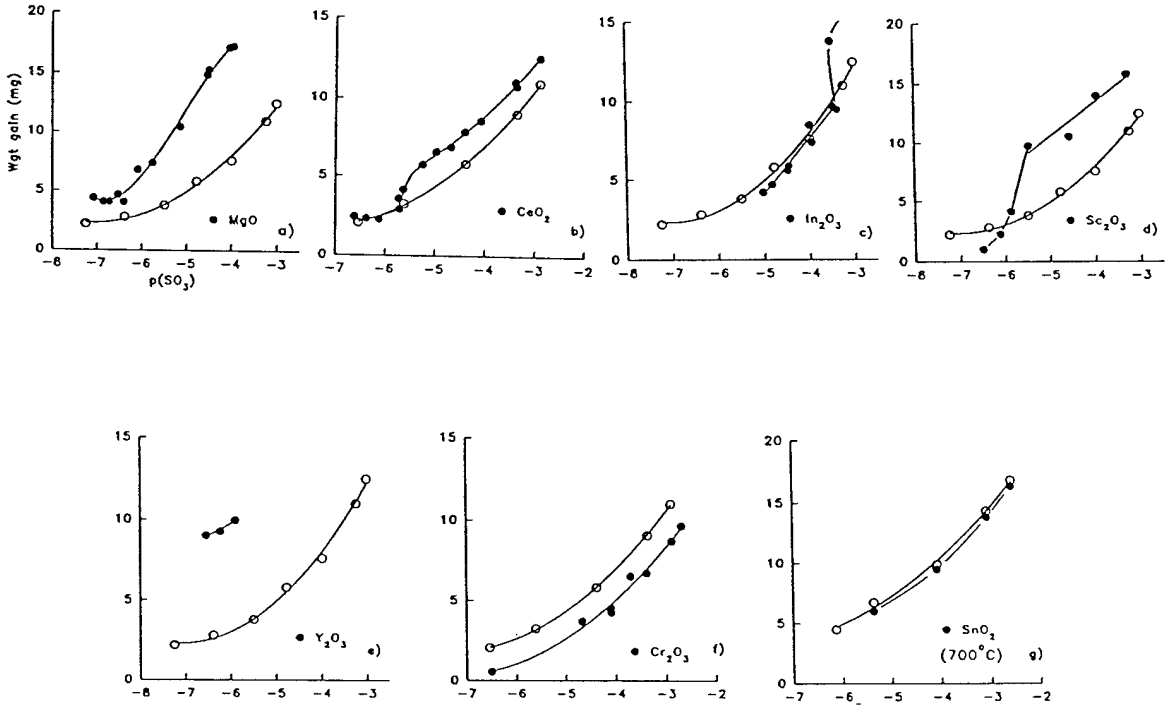

Fig. 10 (a-g) Weight gain vs. $p(SO_3)$ at 800°C for $NaVO_3$ (0.41 mmols) plus various candidate ZrO_2-stabilizing oxides (0.10 mmols).

Formation of soluble product. This is exemplified by MgO (Fig. 10a), where even at a $p(SO_3)$ of 10^{-7} bar, the MgO-$NaVO_3$ mix shows a higher weight gain than for pure $NaVO_3$, even though the amount of $NaVO_3$ is the same in each case. The additional weight gain must come from the uptake of SO_3 by either MgO or Na_2O, since vanadyl sulfate is ruled out at such low $p(SO_3)$. Low melting mixtures of V_2O_6-($2MgO.Na_2O$) or V_2O_6-($MgO.Na_2O$) can form (35), but these would yield no change in weight. Also, thermodynamic calculations indicate that the displacement of Na_2O by MgO by, e.g.,

$MgO + Na_2O.V_2O_6 \rightarrow Na_2O + MgO.V_2O_6$, is highly unfavored. Solid $MgSO_4$ also appears not to be possible, since a critical $p(SO_3)$ of 1.6×10^{-6} bar is indicated for MgO (s) + $SO_3 \rightarrow MgSO_4$ (s) at 800°C. However, if soluble $MgSO_4$ is formed, then appreciable $MgSO_4$ could be produced even at $p(SO_3) \sim 10^{-7}$ bar. Moreover, since such a system would have two degrees of freedom by the phase rule, some $MgSO_4$ (l) can be formed no matter how low the $p(SO_3)$; i.e., there will be no one critical $p(SO_3)$ for onset of reaction. The hypothesis of a soluble $MgSO_4$ product is consistent also with the $MgO\text{-}ZrO_2$ TBC burner rig tests (12) burning Na,V,S-containing fuel, where major amounts of $MgSO_4$ but only minor amounts of Mg vanadate were found on the TBC surface. At the higher $p(SO_3)$ values in Fig. 10a, there is an upturn in weight gain which presumably reflects the onset of magnesium vanadate formation, since the reaction, $2MgO + V_2O_6 = 2MgO.V_2O_6$ is thermodynamically predicted to be possible at 800°C at act.$(V_2O_6) = 8 \times 10^{-5}$ bar. This could not be confirmed unequivocally by x-ray diffraction, however, which in this case gave complex and diffuse patterns (common for Na/Mg vanadate-sulfate phases from melts). Nonetheless, taken overall, the weight gain behavior in Fig. 10a indicates that melt-soluble $MgSO_4$ is formed at low $p(SO_3)$ in the $MgO\text{-}NaVO_3\text{-}SO_3$ system, but that Mg vanadate may be produced at high $p(SO_3)$ (i.e., at high V_2O_6 melt activities).

Metal vanadate formation once critical V_2O_6 activity reached. This behavior is shown by CeO_2 (Fig. 10b), In_2O_3 (Fig. 10c), and Sc_2O_3 (Fig. 10d), although the case for Sc_2O_3 is complicated by the occurrence of $3NaVO_3.Sc_2O_3$. With CeO_2 and In_2O_3, the weight gain curve is just the same as pure $NaVO_3$ (in other words, the oxide is as chemically inert as the Pt planchet itself) up to a critical $p(SO_3)$, where the melt V_2O_6 activity is raised (via reaction 12) sufficiently that the oxide begins to react with V_2O_6 to form the vanadate. The weight gain for CeO_2 and In_2O_3 is then almost vertical, reflecting the insolubility of the vanadate product. Since the rare earth oxides and their vanadates are high-melting compounds with excellent x-ray diffraction patterns, one can show by x-ray, as for CeO_2 and $CeVO_4$ (see below), that only oxide exists below, and only vanadate above, the critical $p(SO_3)$, or actually V_2O_6 activity.

With Sc_2O_3, the weight gain curve for $Sc_2O_3\text{-}NaVO_3$ is <u>below</u> that of $NaVO_3$ up to the critical $p(SO_3)$. Although not originally understood (32), this behavior results because, at temperatures below 880°C (20), Sc_2O_3 reacts with $NaVO_3$ to give the weak compound, $3NaVO_3.Sc_2O_3$. This compound reduces the activity of Na_2O, and therefore less SO_3 is taken up than with pure $NaVO_3$ of equivalent weight. The weight gain rise leans somewhat from the vertical in this case, which possibly reflects the "breaking" of the $3NaVO_3.Sc_2O_3$ compound as $p(SO_3)$ increases. Also, our initial X-ray analysis was in error, with $ScVO_4$ being correctly identified as the only scandium compound above the critical $p(SO_3)$, but Sc_2O_3 as the compound below, when in fact it was $3NaVO_3.Sc_2O_3$. The difficulty in distinguishing between Sc_2O_3 mixed with $NaVO_3$ and $3NaVO_3.Sc_2O_3$ arises because all of the strong peaks for Sc_2O_3 (x-ray standard pattern JCPDS 42-1463) are also contained in the $3NaVO_3.Sc_2O_3$ x-ray pattern (JCPDS 30-1241).

Direct reaction with pure $NaVO_3$. In Fig. 10e, Y_2O_3 is sufficiently basic that it reacts directly with molten $NaVO_3$ to produce YVO_4, which leaves the melt enriched in Na_2O. Therefore, when this system is equilibrated with even very low $p(SO_3)$, there is a high weight gain because of the pre-existing "reservoir" of Na_2O.

Another type of direct reaction occurs with Cr_2O_3 (Fig. 10f) which reacts with pure $NaVO_3$ and reduces the activity of Na_2O, probably by Na_2CrO_4 formation. This then yields less uptake of SO_3 than would be found with pure $NaVO_3$ alone, and over a wide $p(SO_3)$ range.

Inert to the $NaVO_3\text{-}SO_3$ system. Finally, SnO_2 (Fig. 10g) is chemically inert to the $NaVO_3\text{-}SO_3$ system, with the weight gain being essentially identical to that for $NaVO_3$ alone up to at least 1×10^{-3} bar of SO_3. The resistance of SnO_2 to reaction with V_2O_6 may be one reason for its effectiveness in passivating fluid cracking catalysts against deactivation by vanadium impurities in crude oil (7).

Determining Act.(V_2O_5) without Assumption as to Act.(Na_2SO_4)

In calculating act.(V_2O_5) from the $NaVO_3$-SO_3 equilibrium weight gain data via equation [13], one is ultimately dealing with the activity product, act.(V_2O_5) x act.(Na_2SO_4), and an assumption concerning the Na_2SO_4 solution behavior (ideal or nonideal, and what activity coefficient?) must be made to obtain act.(V_2O_5). However, an alternative derivation of act.(V_2O_5), or more specifically, of $\gamma(V_2O_5)$, that is not dependent upon act.(Na_2SO_4) can be made on the basis of reaction [6],

$$2\ CeO_2\ (s) + V_2O_5\ (l) \rightarrow 2\ CeVO_4\ (s) + 1/2\ O_2\ (g) \qquad [6]$$

In this case, CeO_2 and $CeVO_4$ are pure solids of low solubility (24), and $p(O_2)$ is the atmospheric oxygen pressure of 0.21 bar so, at 800°C, the activity of $V_2O_5(l)$ is fixed. Using the thermodynamic data for $CeO_2(s)$, $CeVO_4(s)$ and $V_2O_5(l)$ provided by Yokokawa et al (18), the critical V_2O_5 activity necessary for reaction [6] can be calculated to be 6.2×10^{-4}.

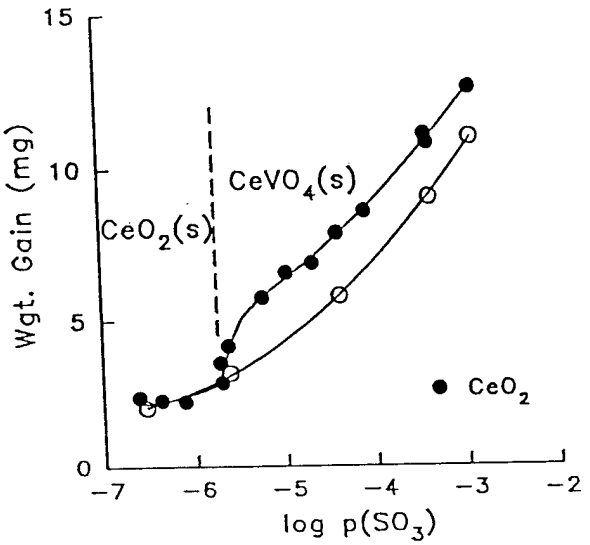

Fig. 11 Weight gain behavior for CeO_2-$NaVO_3$ defining critical $p(SO_3)$ for $CeO_2 \rightarrow CeVO_4$ reaction.

The problem is to identify the V_2O_5 concentration at which reaction [6] just begins. This can be done by examination of Fig. 11, which shows that the weight gain step-up resulting from reaction [6] commences at a $p(SO_3)$ of 3×10^{-6} bar, where the melt weight gain is 3.0 mg, corresponding to formation of 0.091 mol-fraction of V_2O_5 (and Na_2SO_4). If the theoretical V_2O_5 activity for Reaction [6] of 6.2×10^{-4} is divided by the experimental V_2O_5 mol-fraction of 0.091 from Fig. 11, a V_2O_5 activity coefficient of 7×10^{-3} results. This $\gamma(V_2O_5)$ agrees well with the $\gamma(V_2O_5)$-Avg. of ~0.01 indicated in Fig. 9 for $p(SO_3) = 4 \times 10^{-7}$ bar, even though $\gamma(V_2O_5)$, in the present case, is determined on the basis of a different experimental reaction, and without regard to the Na_2SO_4 or $NaVO_3$ solution behavior.

As is well known, calculations such as above depend critically upon the accuracy of the thermodynamic data. Assuming an accumulated ±10 kJ error in $\Delta G°$ for reaction [6] causes the derived $\gamma(V_2O_5)$ to vary from 2.1×10^{-2} to 2.2×10^{-3}. This error bar is shown for the datum point of $\gamma(V_2O_5) = 7 \times 10^{-3}$, $X(V_2O_5) = 0.091$ which has been included as representative of the present experiment for the $\gamma(V_2O_5)$ comparison in Fig. 14 below. It is not an insignificant error, but fits well within the data band. Good agreement is thus seen between two independent sets of experiments (i.e., SO_3-$NaVO_3$ equilibrium, and $CeO_2 \rightarrow CeVO_4$ reaction), in which two different sets of thermodynamic data (Luthra & Spacil, and Yokokawa et al) were used. Error in the thermodynamic data is therefore unlikely to seriously invalidate the present results, especially in their role of serving to indicate the general range of V_2O_5 nonideality in vanadate-sulfate melts.

V_2O_5 Titration using $CeVO_4$ Formation as "Indicator" to Determine $\gamma(V_2O_5)$

Reaction [6] is analogous to the metallurgical reaction,

$$M\ (s) + 1/2\ O_2\ (g) \rightleftarrows MO\ (s) \qquad [16]$$

which has great significance in metallurgy. By reaction [16], one can, for a given temperature, determine either $\Delta_f G°$ for MO, or the critical $p(O_2)$ for metal oxidation/reduction, provided that the other is known. Moreover, reaction [16] is totally independent of the gaseous environment. Large quantities of inert gases such as nitrogen or argon can be present, and there can be other reactions in which O_2 engages (e.g., $CO + 1/2\ O2 = CO_2$) but, if obeyed as written, reaction [16] will nonetheless remain independent.

For the case of reaction [6], a critical V_2O_6 (l) activity of 6.2×10^{-4} is required at 800°C, according to calculations based on the thermodynamic data of Yokokawa et al (18), for the reaction to proceed,

$$2\ CeO_2\ (s) + V_2O_6\ (l) \rightleftarrows 2\ CeVO_4\ (s) + 1/2\ O_2\ (g) \qquad [6]$$

If obeyed as written, reaction [6] is independent of the melt composition, and the V_2O_6 (l) activity required for reaction [6] will always, at 800°C, be 6.2×10^{-4} regardless of melt composition. However, the V_2O_6 activity coefficient can, and most probably will, change with melt composition. Therefore, by finding the mol-fraction of V_2O_6 at which reaction [6] commences, one can potentially determine $\gamma(V_2O_6)$ for virtually any melt system in which an appropriate V_2O_6 activity for reaction [6] to proceed can be attained.

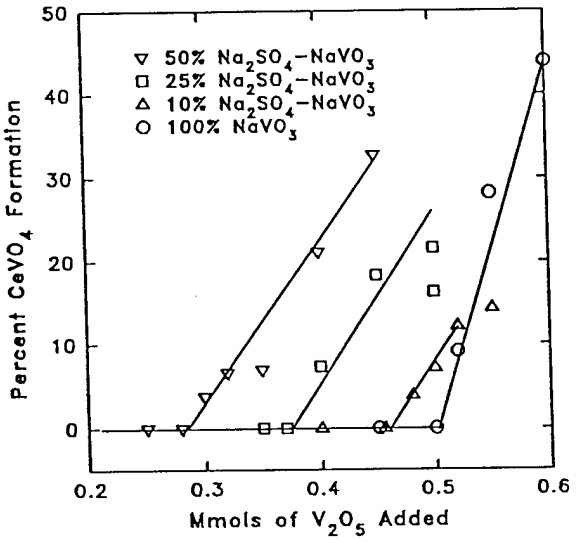

Fig. 12 Mmols V_2O_6 required for $CeVO_4$ formation at 800°C vs. $NaVO_3$-Na_2SO_4 melt composition.

This idea was tested using melts consisting of 1 mmol of CeO_2 mixed with 4 mmol blends of vanadate-sulfate of four different compositions, viz., 100% $NaVO_3$, $NaVO_3$-(10 mol%)Na_2SO_4, $NaVO_3$-(25 mol%)Na_2SO_4, and $NaVO_3$-(50 mol%)Na_2SO_4. A series of varying amounts of V_2O_6 were added to the melt mixes, which were then heated at 800°C for 2 hrs in quiescent air and x-rayed to determine the amount of $CeVO_4$ formed. The relative amount of $CeVO_4$ produced was determined via the expression,

$$\%\ CeVO_4 = 100 \times \frac{[CeVO_4(200)\ \text{Peak Hgt.}]}{[CeVO_4(200)\ \text{Peak Hgt.}] + [CeO_2(111)\ \text{Peak Hgt.}]} \qquad [17]$$

which is an approximation of the integrated intensity ratio formulation commonly used to determine the relative amounts of crystal phases by x-ray diffraction (36). By extrapolation of the percent of $CeVO_4$ formation to zero (Fig. 13), one can ascertain the mmols of V_2O_6 that must be added to raise the melt V_2O_6 activity to the point at which $CeVO_4$ formation begins, and CeO_2(s), $CeVO_4$(s), V_2O_6(l), and atmospheric O_2 are all in equilibrium; that is, when reaction [6] is obeyed.

The results yielded from Fig. 12 are tabulated in Table 3, where the calculated $\gamma(V_2O_6)$ is 6×10^{-3} for $NaVO_3$-(10 mol%)Na_2SO_4 to which 0.1031 $X(V_2O_6)$ had been added. This $X(V_2O_6)$ is near the 0.0853 $X(V_2O_6)$ obtained by equilibrating $NaVO_3$ under 4.1×10^{-7} bar of SO_3 (cf. Table 2), and where $\gamma(V_2O_6)$-Approx.2 was 3.6×10^{-3}. To obtain a better comparison, the data in Table 2 were linearly interpolated to 0.1031 $X(V_2O_6)$, which yielded a value for $\gamma(V_2O_6)$-Approx.2 of 9.1×10^{-3}. This latter $\gamma(V_2O_6)$ of 9.1×10^{-3} agrees well the $\gamma(V_2O_6)$ of 6×10^{-3} from Table 3, especially considering that a

linear interpolation was applied to the Table 2 data. A datum point of $\gamma(V_2O_6) = 6 \times 10^{-3}$, $X(V_2O_6) = 0.1031$ with an error bar corresponding to ± 10 kJ error in $\Delta G°_{reaction}$, which is still the largest likely error, is included in Fig. 14 as representative of this experiment. As shown in the drawn square in Fig. 14, the three independent experimental techniques all give essentially the same $\gamma(V_2O_6)$ for V_2O_6 in the 0.1 mol-fraction concentration range.

TABLE 3

Millimoles of V_2O_6 Required for $CeVO_4$ Formation
as a Function of Na_2SO_4 Content of the Melt at 800°C

Nominal melt composition	Mmols V_2O_6 for $CeVO_4$ formation	Mol-fraction of V_2O_6	Final mol-fraction of Na_2SO_4	Act. Coeff.[1] of V_2O_6
100% $NaVO_3$	0.51	0.1131	0.0	0.0055
$NaVO_3$-(10 mol%)Na_2SO_4	0.46	0.1031	0.0897	0.0060
$NaVO_3$-(25 mol%)Na_2SO_4	0.38	0.0868	0.2283	0.0071
$NaVO_3$-(50 mol%)Na_2SO_4	0.29	0.0676	0.4662	0.0092

[1] Calculated for act.$(V_2O_6) = 6.2 \times 10^{-4}$

When V_2O_6 is added to melts containing significant Na_2SO_4, the back-reaction of Reaction [12] can occur, with $NaVO_3$ produced in the melt and SO_3 evolved. In a flowing air stream, where SO_3 is continually removed, there can be a major extent of back-reaction, with 50 mol% Na_2SO_4-$NaVO_3$ being converted ~80% to $NaVO_3$ in 24 hrs at 750°C [19]. In quiescent furnace air, the degree of back-reaction is much less. Also the reaction kinetics are slow in comparison to most chemical reactions. In the present case, the CeO_2 is finely ground together and thoroughly mixed with the $NaVO_3$-Na_2SO_4-V_2O_6 blend before firing. Upon coming to temperature, there is rapid reaction to form stable $CeVO_4$, and since the CeO_2 is in excess of V_2O_6, no residual V_2O_6 is left to undergo reaction with Na_2SO_4 in the melt (which is heated only 2 hrs). Error because of Na_2SO_4 reaction with residual V_2O_6 should therefore be negligible.

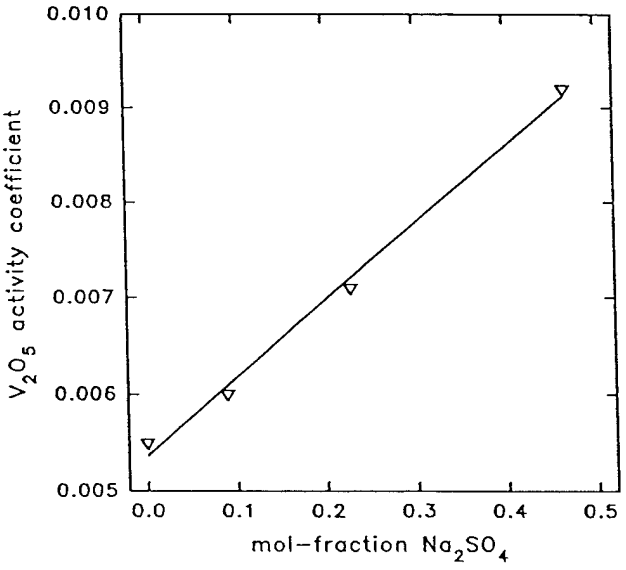

Fig. 13 Activity coefficient of V_2O_6 vs. mol-fraction of Na_2SO_4 at 800°C.

When the V_2O_6 activity coefficients from Table 3 are plotted against the mol-fraction of Na_2SO_4, an essentially straight line is obtained (Fig. 13). Theoretical reasons as to why the line should be straight have not been developed. However, Figs. 12 and 13 contain two points which have not been explicitly shown before, and which are perhaps not intuitive. First, increasing the Na_2SO_4 content of the melt causes $\gamma(V_2O_6)$ to increase; that is, V_2O_6 reaction with CeO_2 (and presumably other ceramic oxides) occurs with less V_2O_6 required in the melt (or vanadium in the fuel). Second, small differences in the V_2O_6 activity coefficients are not negligible. A change in $\gamma(V_2O_6)$ of from 5.5×10^{-3} to $9.2 \times ^{-3}$, although at first sight insignificant, in fact corresponds to a nearly 2X decrease from 0.51 mmols to

0.29 mmols in the amount of V_2O_6 required to reach the melt V_2O_6 activity at which CeO_2 will react or "corrode". In the service world, this could mean having to buy a fuel of half the vanadium content at considerably more expense.

SUMMARY AND CONCLUSIONS

Comparison with V_2O_6 Activity Coefficients from the Literature

The known V_2O_6 activity coefficients that have been reported for sodium vanadate, and sodium vanadate-sulfate mixtures, are shown in Fig. 14. The comparison is only qualitative, since the activity coefficients were measured with different melt conditions and temperatures. The Mittal and Elliott data point is calculated from their measurement of the activity of V_2O_6 in 0.5 mol-fraction $Na_2O.V_2O_6$ (i.e., $NaVO_3$) at 850°C. The two Luthra and Spacil data points were reported for melts having a Na/V ratio of 2, and equilibrated under $p(SO_3)$'s of approximately 9×10^{-4} and 4×10^{-4} atm at 750°C and 900°C, respectively. Although Hwang and Rapp (23) originally postulated sodium sulfate-vanadate solutions to be ideal, a later paper by Rapp and Zhang (37) describes the equilibration of Na_2SO_4-V_2O_6 melts of varying Na/V ratio under a fixed $p(SO_3)$ of 2.2×10^{-3} bar at 900°C, and concludes that the melts are "--close to an ideal salt solution although a small deviation seems to be present." No activity coefficient for V_2O_6 is given in their paper, but in a review of an NRL manuscript on vanadate-sulfates, a reviewer who seemed quite knowledgeable about the work stated that a V_2O_6 activity coefficient of 0.79 was indicated by the Rapp and Zhang results. So, despite its unusual derivation, this $\gamma(V_2O_6)$ is plotted in Fig. 14 for completeness of the comparison.

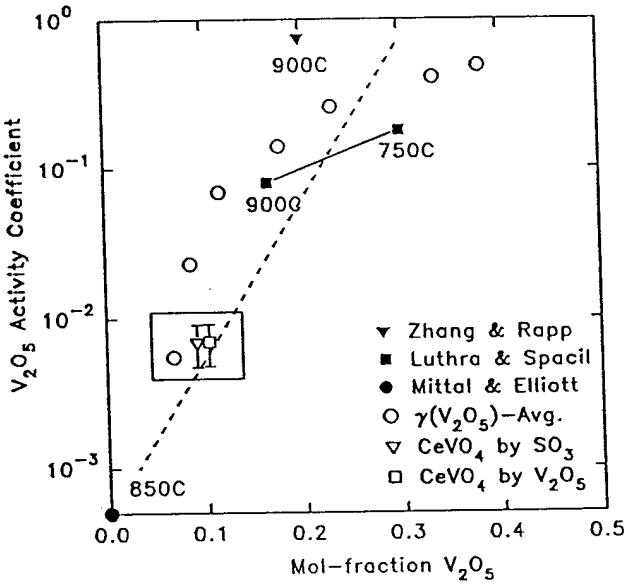

Fig. 14 Comparison of V_2O_6 activity coefficients from various works as plotted vs. mol-fraction of melt V_2O_6.

Although somewhat scattered, the data in Fig. 14 exhibit a general trend of increase in $\gamma(V_2O_6)$ as the mol-fraction of V_2O_6 increases. Despite the difference in temperature, there is an essentially smooth transition between the $\gamma(V_2O_6)$ of $\sim 5 \times 10^{-4}$ (or $10^{-3.3}$) indicated by the Mittal and Elliott data for pure $NaVO_3$ at 850°C, and the $\gamma(V_2O_6)$ of $\sim 5 \times 10^{-3}$ determined from NRL results for an 800°C $NaVO_3$ melt containing 0.067 mol-fraction each of Na_2SO_4 and V_2O_6. This is consistent with our expectations, considering that at this point only small increments of V_2O_6 have been added to pure $NaVO_3$. There is also reasonably good agreement with the Luthra and Spacil V_2O_6 activity coefficients of 0.08 and 0.18 in the middle regions of the plot, and with the 0.79 V_2O_6 activity coefficient of Rapp and Zhang for Na/V melts under high SO_3 partial pressures.

The three datum points within the drawn square are of particular importance. As described above, these points were determined by three independent experimental techniques, viz., simple equilibrium of $NaVO_3$ under SO_3; the reaction $CeO_2 + V_2O_6 \rightarrow CeVO_4 + 1/2\ O_2$ where the V_2O_6 melt activity was increased by raising $p(SO_3)$; and the same reaction where V_2O_6 was simply "titrated" into the melt. Two different sets of thermodynamic data were also employed. Good agreement is seen

between the three values for $\gamma(V_2O_6)$ so obtained, which gives confidence that our experiments and data are essentially correct.

Other considerations

Effect of Na/V ratio in melt or engine deposit. In addition to $p(SO_3)$, the other principal variable in the Na_2O-V_2O_6-SO_3 system is the Na/V ratio. Information on the effect of the Na/V ratio is contained in our V_2O_6 "titration" experiments where blends of different $NaVO_3$-Na_2SO_4 ratios were investigated. For example, $NaVO_3$-(50 mol%)Na_2SO_4 has a Na/V ratio of 3, and could be considered as approximating a melt that was originally Na_2O-(50 mol%)$NaVO_3$ (or Na_3VO_4), but in which the Na_2O component has been sulfated. Such an assumption is not unreasonable, since Na_2O has a considerably higher affinity for SO_3 than for V_2O_6, as evidenced by the fact that the 800°C Na_2SO_4 dissociation activity product, act.(Na_2O) x act.(SO_3), is 9.8×10^{-21}, whereas the equivalent activity product for $NaVO_3$, act.(Na_2O) x act.(V_2O_6), is 1.7×10^{-18}. Taking this model to be indicative even if not totally correct, one can interpret the data in Fig. 13 as being for melts of Na/V ratios of 1, 1.22, 1.67 and 3.0, respectively, wherein $\gamma(V_2O_6)$ is found to progressively increase from 5.5×10^{-3} to 9.2×10^{-3}, or by 67%. Compared to the large changes in $\gamma(V_2O_6)$ produced by increasing $p(SO_3)$, this is relatively small, which suggests that $\gamma(V_2O_6)$ is not highly dependent upon the melt Na/V ratio, at least over the concentration ranges covered.

Vanadate-sulfate melts, ideal or nonideal? The data in Fig. 14 demonstrate that vanadate-sulfate melts are nonideal, and in fact follow a very common solution behavior wherein the melt components, when present in high concentration, behave as "nearly ideal", but when in dilute concentration, exhibit large negative deviations from ideal behavior, and have small activity coefficients.

ACKNOWLEDGEMENTS

The majority of our work was sponsored by the Office of Naval Research, with Dr. A. J. Sedriks as Scientific Officer. The financial support and intellectual encouragement that has been given in conjunction with this effort is gratefully acknowledged.

REFERENCES

1. W. T. Reid, *External Corrosion and Deposits: Boilers and Gas Turbines*, pgs. 134-138, American Elsevier, New York, 1971.

2. R. A. Miller, *Surf. Coat. Technol. 30*[1], 1 (1987).

3. R. L. Jones, "Thermal Barrier Coatings", in *Metallurgical and Ceramic Protective Coatings*, (ed. K. H. Stern), Chapman & Hall, New York, 1996.

4. W. P. Parks, E. E. Hoffman, W. Y. Lee and I. G. Wright, "Thermal Barrier Coatings Issues in Advanced Land-Based Gas Turbines," in *Proc. of Thermal Barrier Coating Workshop*, pg. 35-47, NASA Conf. Publ. 3312, NASA Lewis Research Center, OH (1995).

5. *Proc. of the Advanced Turbine Systems Annual Program Review Meeting*, DOE/OR-2048, (eds. A. Layne and P. Hoffman) U.S. Dept. of Energy, Washington DC, Nov., 1996.

6. J. F. Branthaver, "Influence of Metal Complexes in Fossil Fuels on Industrial Operations," in *Metal Complexes in Fossil Fuels: Geochemistry, Characterization and Processing*, pgs. 188-204 (eds. R. H. Filby and J. F. Branthaver) ACS Symp. Series 344, American Chemical Society, Washington, DC, 1987

7. R. L. Jones, *J. of Catalysis, **129**,* 269 (1991).

8. H. E. Hilliard, "Vanadium", in *Mineral Commodity Summaries, 1997*, U.S. Dept. of Interior, U. S. Geological Survey, Reston, VA, 1997.

9. *Proc. of 1st Conf. on Advanced Materials for Alternative Fuel Capable Directly Fired Heat Engines*, (eds. J. W. Fairbanks and J. Stringer), CONF-790749, U.S. Dept. of Energy, Washington, DC, 1979.

10. *Proc. of the 2nd Conf. on Advanced Materials for Alternative-Fuel-Capable Heat Engines*, (eds. J. W. Fairbanks and J. Stringer), RD-2369-SR, Electric Power Research Institute, Palo Alto, CA, 1982.

11. B. A. Nagaraj, A. F. Maricocchi, D. J. Wortman, J. S. Patton and R. L. Clarke, *ASME Paper 92-GT-44*, American Society of Mechanical Engineers, New York, 1992.

12. B. A. Nagaraj and D. W. Wortman, *Trans. ASME, J. Engr. for Gas Turbines and Power, **112**,* 536 (1990).

13. R. L. Jones, *J. Thermal Spray Technol., **6***[1], 77 (1997).

14. R. L. Jones, *Surf. Coat. Technol., **39/40**,* 89 (1989).

15. D. W. Susnitzky, W. Hertl and C. B. Carter, *J. Am. Ceram. Soc., **71***[11], 992 (1988).

16. W. Hertl, *J. Appl. Phys., **63***[11], 5514 (1988).

17. A. N. Belov and G. A. Semenov, *Russ. J. Physical Chemistry, **59***[3], 342 (1985).

18. H. Yokokawa, N. Sakai, T. Kawada and M. Dokiya, *J. Am. Ceram. Soc., **73***[3], 649 (1990).

19. R. L. Jones, C. E. Williams and S. R. Jones, *J. Electrochem. Soc., **133***[1], 227 (1986).

20. V. H. Schwarz and L. Schmidt, *Z. anorg. allg. Chem., **413**,* 150 (1975).

21. K. L. Luthra and H. S. Spacil, *J. Electrochem. Soc., **129***[3], 649 (1982).

22. S. K. Mittal and J. F. Elliott, *J. Electrochem. Soc., **131***[5], 1194 (1984).

23. Y.-S. Hwang and R. A. Rapp, *Corrosion, **45***[11], 933 (1989).

24. R. F. Reidy and R. L. Jones, *J. Electrochem. Soc., **142***[4], 1353 (1995).

25. M. Chaikivsky and C. W. Siegmund, *ASME Trans., J. Engr. for Power, **87**,* Series A, 379 (1965).

26. A. Block-Bolton and D. R. Sadoway, *Metall. Trans. B, **14**,* 231 (1983).

27. R. Mittelstadt and K. Schwerdtfeger, *Metall. Trans., 21B*, 111 (1990).

28. R. F. Reidy and K. E. Swider, *J. Am. Ceram. Soc., 78*[4], 1121 (1995).

29. D. W. Bonnell and J. W. Hastie, *High Temp. Science, 26*, 313 (1990).

30. Y. K. Rao, *Stoichiometry and Thermodynamics of Metallurgical Processes*, pg. 825, Cambridge University Press, Cambridge, 1985.

31. "Phase diagram for V_2O_5-Na_2O System", Fig. 5126, *Phase Diagrams for Ceramists, Vol. IV*, (ed. G. Smith), The American Ceramic Society, Columbus, OH, 1981.

32. I. Barin, *Thermochemical Data of Pure Substances*, VCH Verlags Gesellschaft, Weinheim, 1989. As given in the commercial computer program, HSC Chemistry for Windows (Version 2.03)™.

33. R. L. Jones, *J. Electrochem. Soc., 139*[10], 2794 (1992).

34. R. L. Jones, *J. Am. Ceram. Soc., 76*[6], 1635 (1993).

35. R. C. Kerby and J. R. Wilson, *Can. J. Chem., 51*, 1032 (1973).

36. H. K. Schmidt, *J. Am. Ceram. Soc., 70*[5], 367 (1987).

37. R. A. Rapp and Y. S. Zhang, "Electrochemical Studies of Hot Corrosion of Materials," in *Proc. of 1st Mexican Symp. on Metallic Corrosion*, Paper 12, pgs. 90-99, Meridan, Mexico, 7-11 March, 1994.